Journal of Quantitative Spectroscopy & Radiative Transfer 113 (2012) 461–469

Contents lists available at SciVerse ScienceDirect

Journal of Quantitative Spectroscopy & Radiative Transfer

journal homepage: www.elsevier.com/locate/jqsrt

Effects of stratocumulus, cumulus, and cirrus clouds on the UV-B diffuse to global ratio: Experimental and modeling results

María Laura López*, Gustavo G. Palancar*, Beatriz M. Toselli

Departamento de Físico Química/INFIQC/Centro Láser de Ciencias Moleculares, Facultad de Ciencias Químicas, Universidad Nacional de Córdoba, Ciudad Universitaria, 5000 Córdoba, Argentina

ARTICLE INFO

Article history:
Received 15 September 2011
Received in revised form
27 December 2011
Accepted 28 December 2011
Available online 5 January 2012

Keywords:
Types of clouds
DGR
UV-B irradiance
Radiative transfer model
Cloud optical properties

ABSTRACT

Broadband measurements of global and diffuse UV-B irradiance (280–315 nm) together with modeled and measured diffuse to global ratios (DGR) have been used to characterize the influence of different types of clouds on irradiance at the surface. Measurements were carried out during 2000–2001 in Córdoba City, Argentina. The Tropospheric Ultraviolet Visible (TUV) model was used to analyze the behavior of the modeled DGRs for different cloud optical depths and at different altitudes and solar zenith angles (SZA). Different cloud altitudes were also tested, although only the results for a cloud placed at 1.5–2.5 km of altitude are shown. A total of 16 day with stratocumulus, 12 with cumulus, and 16 with cirrus have been studied and compared among them and also against 21 clear sky days. Different behaviors were clearly detected and also differentiated through the analysis of the averages and the standard deviations of the DGRs: 1.02 ± 0.06 for stratocumulus, 0.74 ± 0.18 for cumulus, 0.63 ± 0.12 for cirrus, and 0.60 ± 0.13 for the clear sky days, respectively. Stratocumulus clouds showed a low variability in the DGR values, which were concentrated close to one at all SZAs. DGR values for cumulus clouds presented a large variability at all SZAs, mostly associated with the different optical depths. Finally, the closeness between the DGR values for cirrus clouds and the DGR values for clear days showed that these clouds generally do not strongly affect the UV-B irradiance at the surface at any SZA. In the opposite side, stratocumulus clouds were identified as those with the largest effects, at all SZAs, on the UV-B irradiance at the surface.

1. Introduction

Tropospheric chemistry is mainly driven by the photodissociation of ozone, aldehydes, and peroxides (producing OH and OH_2 radicals) and by the photolysis of NO_2 (controlling the NO/NO_2 balance). As the photolysis rates depend on the amount of radiation (especially UV), the study of its levels and distribution is essential to quantitatively understand the photochemistry in the troposphere.

The UV radiation components (diffuse and direct irradiances) at ground level depend on various temporal, spatial and meteorological factors such as solar zenith angle (SZA), season, aerosol loading and properties, cloudiness, ozone amount, site altitude, surface albedo, etc [1]. However, the attenuation of UV-B radiation by clouds is frequently larger than any other atmospheric parameter. The effect of clouds on instantaneous UV-B levels can vary from small enhancements to almost total reduction [2]. Atmospheric aerosols also affect UV-B radiation, although in a reduced amount in comparison with clouds [3]. Cloud macrophysical structures (three-dimensional geometry, type and pattern) and their microphysical properties (liquid/ice water content, particle effective sizes, and

* Corresponding authors. Fax: +54 351 4334188.
E-mail addresses: llopez@fcq.unc.edu.ar (M.L. López), palancar@fcq.unc.edu.ar (G.G. Palancar).

0022-4073/$ - see front matter © 2012 Elsevier Ltd. All rights reserved.
doi:10.1016/j.jqsrt.2011.12.018

distribution of water/ice particles) determine their optical characteristics, which affect absorption and scattering of solar radiation. The scattering processes lead to an increased path length of the photons while absorption results in a loss of photons. Both processes affect photolysis rates. The most challenging problem in cloud studies is that their macro and microphysical properties are highly variable in space and time [4,5]. These variations are responsible for the great variability observed in UV radiation under cloudy skies.

Different theoretical and empirical parameterizations have been proposed to quantify the effect of clouds on UV radiation. One of them is the Cloud Modification Factor (CMF) defined as the ratio between the measured radiation in a cloudy sky and the calculated radiation for a cloudless sky [6–10]. Another used parameter, equivalent to the CMF, is the transmission factor, defined as the ratio of the cloudy actinic flux at a certain wavelength to that under cloudless conditions at the same SZA [11].

The relation between the radiation components is also used to quantify the effect of clouds. Ogunjobi et al. [12] investigated the effect of the total optical depth and cloud cover on the diffuse and direct components of solar radiation in the spectral range 400–940 nm. They found that when the cloud cover is small the fractions of the direct and diffuse components were 0.66 and 0.34 of the global component, respectively. However, under highly cloudy conditions the diffuse and direct fractions were 0.98 and 0.02, respectively. Jacovides et al. [13] linked the global and diffuse solar irradiances (305–2800 nm) with the photosynthetic photon flux density (global and diffuse) and used these data to calculate the ratios and determine their temporal variability and their dependence on sky conditions. Kaskaoutis et al. [14] used the diffuse to global irradiance ratio (DGR) as a cloud-screening criterion. Harrison et al. [15] measured global and diffuse solar irradiance and calculated the diffuse/global ratio. They compared these ratios with subjective cloud observations finding that the ratios are sensitive to cloud amount, particularly for low and moderate cloud coverage. They report that the ratio is equal to 1 in overcast conditions and found that the variability in the diffuse/global ratios provides basic information on cloud type: large variations indicate the presence of convective clouds and small variations occur under stratiform clouds. Long and Ackerman [16] developed an automated method to identify clear-sky periods by using downwelling total and diffuse irradiances and their normalized ratio (DGR). In that work they use a series of four tests to eliminate data that occur under cloudy skies.

The distribution of the radiation in its components depends on parameters that are altitude dependent. Thus, the altitude dependence of the photolysis rates should also be taken into account for precise model calculation of production rates and mixing ratios of photochemical secondary compounds [17,18]. One of the parameters that affect the radiation is the vertical distribution of water and ice in stratiform and cumuliform cloud fields [19]. Different works report this effect of clouds on the vertical profile of the radiation. Junkermann [17] investigated the vertical distribution of the UV actinic radiation under aerosol and cloud presence. He found that the effects of scattered convective clouds were often masked by aerosols and the aerosol content was generally the dominating factor controlling radiation transfer. Pfister et al. [20] studied the influence of clouds on the vertical profile of the O_3 and NO_2 photolysis rate coefficients. They used radiative transfer model calculations and aircraft measurements and found that the actinic flux is generally lower below clouds compared to clear-sky values, but shows an increase inside and a large enhancement above clouds.

Radiative transfer models are extensively used to assess the effects of clouds on radiation. Nevertheless, the validity of their results is closely related to the approximations they make to represent the complexity of the clouds. Because of that, the comparison against experimental measurements becomes not only a useful but also an essential procedure. Studies about radiation-cloud interactions are usually focused on the effects in the visible or infrared ranges, although, from the point of view of photolysis processes, the UV range is the most important. Because of all this, the present work was aimed to highlight the importance of the effects of the different types of clouds on the distribution of the surface UV-B irradiance by using both approaches: experimental measurements and model calculations. Thus, this work analyzes these effects through measured and modeled DGRs under different conditions. Ratios were calculated for stratocumulus, cumulus and cirrus clouds, because these kinds of clouds are the most common at Córdoba City. In order to comprehensively understand the variation of the DGR during the day and also in altitude, model calculations were performed by using an infinite homogeneous plane parallel cloud with different optical depths. Clear sky DGRs were also measured and calculated to be used as a reference. In this work, Section 2 describes the data collection, Section 3 the model setup, and Section 4 the correction procedure applied to the diffuse measurements. Section 5 shows the results and Section 6 summaries the main conclusions.

2. Data

The instruments used in this work are a YES (Yankee Environmental System, Inc.) pyranometer model TSP-700 and two YES model UVB-1 pyranometers. The TSP-700 measures total global irradiance (300–3000 nm) while the YES UVB-1 measures UV-B global irradiance (280–315 nm). One of the UVB-1 pyranometers was used to measure UV-B diffuse irradiance, blocking the direct radiation with a home-made shadowband, while the other was used to simultaneously measure the global UV-B irradiance. In order to assure the comparability of both UVB-1 instruments, global irradiances were systematically compared during and after the measurement period. Here it was found that the differences were always within $\pm 2\%$.

The pyranometers were factory calibrated and mounted on a wide-open area at the University Campus in Córdoba City, Argentina (31° 24′ S, 64° 11′ W, 470 m.a.s.l.). Broadband observations were recorded as half a minute average values to capture the fast cloud variability and its corresponding

effects. The measurement site and the instruments have been described in Palancar and Toselli [21].

The broadband measurements were taken during the years 2000 and 2001. Clouds were classified by direct observation as cirrus, cumulus, and stratocumulus. Only measurements affected by one well defined type of cloud were used in this study. Although this greatly reduces the number of available days it assures that the observed effects are due to the type of cloud under study. Here, it has to be assumed that during the measurement period the aerosol optical depth was low and the ozone column remained relatively constant. The first assumption was assured through comparisons against model calculations and visual evaluations of the sky while the second one is supported by previous statistical studies [22].

Total irradiance measurements were used to characterize cloud conditions because visible and infrared wavelengths are more sensitive than the UV-B ones to cloud presence. Besides, thin cirrus clouds can be confused with a high load of aerosols in the UV-B wavelengths.

3. Model calculations

The UV-B calculations were performed with the Tropospheric Ultraviolet and Visible (TUV) radiation model version 4.1 [23]. This model uses the Discrete Ordinate Radiative Transfer Code (DISORT) implementation for the solution of the radiative transfer equation [24]. Model calculations were restricted to the wavelength range between 280 nm and 315 nm using a resolution of 1 nm. The radiative transfer is calculated considering several extinction processes in the atmosphere: Rayleigh scattering, Mie scattering and the absorption due to atmospheric gases. The model incorporates clouds as infinite plane parallel homogeneous layers, simulating overcast conditions. In this work, tropospheric O_3, SO_2 and NO_2 have not been considered in the calculations because they are present in low levels in Córdoba City [25]. However, total ozone column was considered. Daily values were taken from the Total Ozone Mapping Spectrometer (TOMS) webpage and scaled to the ozone profile used in the TUV model. A more detailed description of the setup used in the model can be found in López et al. [7]. In this work, an 8-stream discrete ordinate method was used. Earth atmosphere was divided in 10 equally spaced layers (1 km thick) up to 10 km above ground level. All data correspond to SZA smaller than 70° because of the known uncertainties which affect models and measurements at larger SZAs [22].

4. Diffuse correction

The UV-B diffuse irradiance was measured with one of the UVB-1 pyranometers by blocking the direct beam with a fixed homemade shadowband, which was manually adjusted along the year to consider the variation of the minimum SZA. Given the particular dimensions and setup of the shadowband, which not only obstructs the direct irradiance but also part of the diffuse irradiance, we needed to develop our own correction procedure. This procedure was applied only to correct for the fraction of the UV-B diffuse irradiance blocked by the shadowband during cloudy days. In this method measurements of UV-B diffuse irradiance for 21 clear sky days (i.e., no clouds and no aerosols) were compared with the corresponding modeled irradiances under the same atmospheric conditions. A detailed description of this procedure is given in Appendix A. The validation was done through the comparison between the global and the diffuse irradiances under overcast conditions. Under these conditions, attenuation of direct irradiance is complete and the diffuse and global irradiances are equal [15]. Fig. 1(a) shows the measured global and diffuse UV-B irradiances during a day with stratocumulus in the afternoon. Although DGR values higher than 1 represent unphysical situations (Fig. 1(b)) they are justified considering the involved uncertainties. The total uncertainty includes those related to irradiance measurements (diffuse and global), model calculations, instrument calibration, correction procedure, and also the manual selection of the data affected by each type of cloud. The dominant one is the first one. Overall, notice that under overcast conditions the global irradiance agrees within $\pm 10\%$ of the corrected diffuse irradiance. A few exceptions (the highest DGR values) are due to the uncertainties associated with the absolute differences between very low irradiance values.

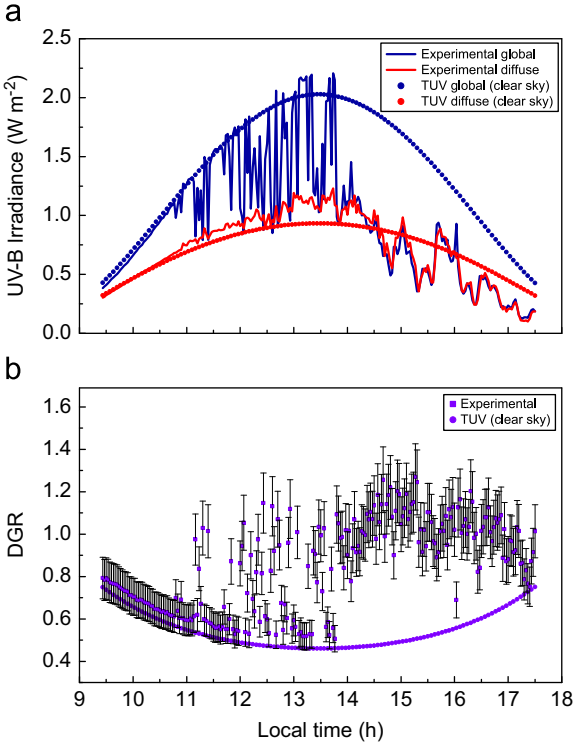

Fig. 1. Effect of cumulus (morning) and stratocumulus (afternoon) clouds on the daily course of (a) modeled (clear sky) and measured diffuse and global irradiance at the surface and (b) the experimental and modeled (clear sky) DGRs. Data corresponds to 8 Mar 2001.

5. Results and discussion

In this work the DGR was specifically defined as

$$DGR = \frac{UVB_{\text{diffuse}}}{UVB_{\text{global}}},$$

where UVB_{diffuse} and UVB_{global} denote diffuse and global UV-B irradiances, respectively.

The studies of the measured and modeled DGR are addressed in Sections 5.1 and 5.2, respectively. In the former, stratocumulus, cumulus, and cirrus clouds are analyzed while in the latter a generic infinite homogeneous plane parallel cloud is considered.

5.1. Measured DGR

DGR was calculated for all days when stratocumulus, cumulus, or cirrus clouds were present. As an example, Fig. 1 shows the global and diffuse irradiance and the DGR calculated as a function of local time for one day with presence of stratocumulus and cumulus clouds. Fig. 2 shows the same as Fig. 1 but for cirrus clouds. Only SZAs smaller than 70° were considered due to the known uncertainties which affect models and measurements at larger SZAs. The smallest SZA on each day is determined by the day of the year and the latitude of Córdoba.

Fig. 1(a) shows the global and diffuse irradiances (modeled and measured) for a day (8 March 2001) with clear sky conditions in the morning, cumulus clouds before solar noon, and stratocumulus clouds in the afternoon. The irradiance values correspond to SZA between 29° and 63°. Data were evaluated with a 30 s resolution but, for the sake of the clarity, Fig. 1(a) shows data every 2 min. In the first 60 min of this figure it can be seen the agreement between measurements and model calculations under clear sky conditions for both diffuse and global irradiances. This fact confirms the validity of the method used to correct the diffuse measurements. When the cumulus clouds are present the typical drops and peaks in the global and diffuse irradiance can be observed. Drops occur when the direct beam is blocked by clouds, while the peaks, especially those where the broken cloud effect is evident, occur due to the enhancement in the diffuse component when the direct beam is not blocked. In the afternoon, the presence of stratocumulus clouds leads to the complete attenuation of the direct beam. Consequently, the measured global irradiance equals the corrected diffuse irradiance. This is, again, a fact that supports the corrected diffuse measurements. Fig. 1(b) shows the corresponding modeled and measured DGRs. The errors in the measured DGRs were propagated by considering the errors in the measured diffuse irradiances. In all the analyzed days, the errors were less than 10%, which is shown in the error bars. Thus, the agreement between the DGRs under clear sky conditions is always better than 10%. In contrast, when cumulus clouds are present, large variations and deviations in the measured DGRs are observed with respect to the modeled DGRs under clear sky conditions. Finally, when stratocumulus clouds are present, the DGR values also show large differences with respect to the clear sky DGRs, but with values close to one. Values larger than one are most likely due to the uncertainties introduced in the correction of the diffuse irradiances. For most of them, the interval determined by the error bars includes DGR values equal to or less than one. It should be also noted that, for this type of cloud, the variability in the DGR values is less than in the cumulus cloud case. This is because the direct beam under a cumulus cloud field is highly variable (due to the holes), whereas it is not under a stratocumulus cloud field (because it is close to zero everywhere).

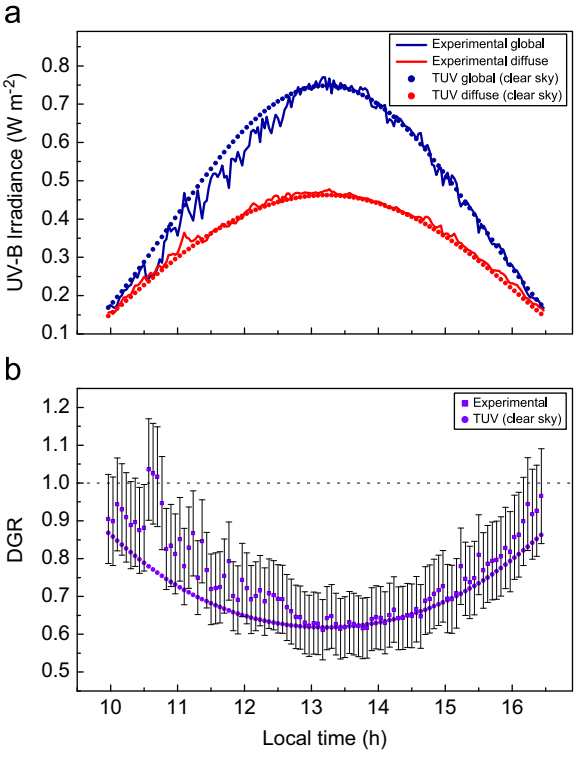

Fig. 2. Same as Fig. 1 but for cirrus clouds. Data corresponds to 22 May 2000.

Fig. 2(a) shows the global and diffuse irradiances (modeled and measured) for a day (22 May 2000) when cirrus clouds were present. The irradiance values correspond to SZA that ranged between 51° and 70°. In the same way as Figs. 1 and 2 shows data with a 2 min time resolution. Fig. 2(b) shows the corresponding modeled and measured DGRs. As cirrus clouds usually have small optical depths, they do not largely affect the UV-B irradiance at the surface. This can be seen in Fig. 2(a) in both diffuse and global irradiances. As a consequence, the measured and modeled DGRs in Fig. 2(b) show an agreement better than 6%. The disagreement observed around 11 a.m. is not a cloud effect but the interference of a building. Figs. 1 and 2 are examples of the calculations that were performed for all the days when a given type of cloud was present. Overall, 16 day with presence of stratocumulus, 12 with cumulus, and 16 with cirrus were analyzed. In total, 5385, 4921, and 6468 measurements, respectively, were used for each condition. SZAs in these measurements ranged from 8° to 70°. Fig. 3 shows the

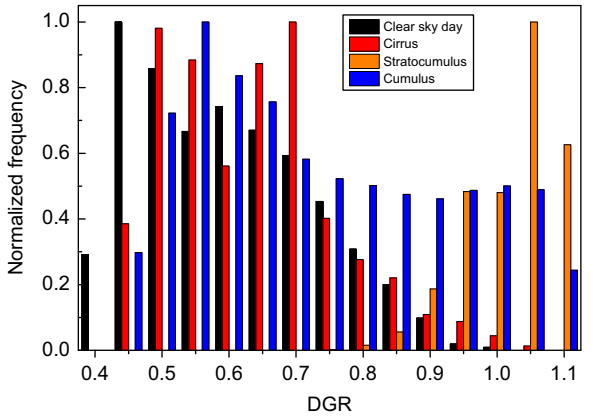

Fig. 3. Frequency distribution (normalized) of the DGR for cumulus, stratocumulus, and cirrus clouds. In order to compare the effects of these clouds the distribution for clear sky days is also included.

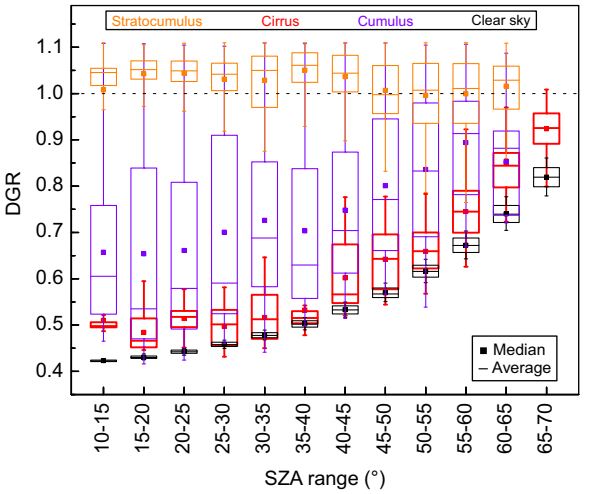

Fig. 4. Box plots of the DGR for cumulus, stratocumulus, and cirrus as a function of different SZA intervals. In order to compare the effects of these clouds the model DGRs for clear sky days are also included.

normalized frequency distribution of measured DGRs, for each type of cloud and also for the modeled clear sky days. In this figure the different behaviors depending on the sky condition can be clearly seen. The relatively large optical depths and the large cloud cover of stratocumulus lead to the complete conversion of the direct beam to diffuse radiation. This makes stratocumulus the type of clouds that most affects the irradiance distribution at surface. That is why DGRs for stratocumulus are almost always close to one. Lower values arise when the sun shines through the holes between the individual cloud elements or when the cloud optical depth (COD) is small. DGRs of cumulus present a completely different behavior. The most frequent value for this type of cloud is 0.55 with an average of 0.6. Note that this peak is observed at a DGR larger but close to the DGR of the peak shown in the clear sky distribution. This is because cumulus clouds often have holes among the cloud elements. If these holes are sufficiently large the DGRs can be similar to those for a clear sky day. The slightly larger average value for the cumulus is because of the cloud-side scattering and the radiation coming from the bottom of these clouds, both contributing to the diffuse component. Contrary to the behavior of stratocumulus, cumulus clouds do not present a clear trend for DGR values larger than 0.7. For DGR values larger than 0.7 all the values are equally frequent. This fact can be explained considering both the different optical depths and also the variability in the radiation paths due to the inhomogeneity in the horizontal and vertical extensions of these clouds. Finally, the distribution of the DGR values for cirrus is similar to that of the clear sky days although slightly shifted toward larger values. The similar behavior is attributed to the small optical depths of these clouds while the shift is because of this extra contribution to the diffuse radiation. Because of these small optical depths, the diffuse component is not enhanced as much as in the cumulus case (see Figs. 1 and 2), although the usual large spatial cover of cirrus partially compensates for this difference. Observe the low frequency of DGRs larger than 0.75. It shows that cirrus is the type of cloud that least affects the irradiance distribution at surface. This conclusion is supported by the analysis of the average and the standard deviation of the DGRs. These values are 0.60 and 0.13 for the clear sky days, 0.63 and 0.12 for cirrus, 0.74 and 0.18 for cumulus, and 1.02 and 0.06 for stratocumulus. Fig. 3 shows a general analysis of the measured DGRs independently of the SZA. To study the SZA dependence, all the DGR values were grouped in SZA intervals of 5°. This procedure was applied to all data of the three types of cloud and also to the modeled data for the clear sky days. Fig. 4 shows the corresponding box plots where the concentration and variability of DGR for the different SZA intervals can be seen. Note that the trend in the boxes can be clearly differentiated among the types of cloud and also between them and the clear sky condition. The analysis for each type of cloud is explained as follows.

5.1.1. *Clear sky day*

For a clear sky day, the behavior of the DGR values during the day is determined by Rayleigh scattering, which is much larger at large SZAs (low sun). Hence, the DGR values increase at larger SZAs. Note that these values determine the lower limit in Fig. 4 as the presence of clouds always increases the diffuse component relative to the global component.

5.1.2. *Stratocumulus*

The small size of the boxes indicates that the variability of the DGRs is low. The values are concentrated close to 1 at all the SZAs. It shows that the effect of stratocumulus on the increase of the diffuse irradiance relative to the global irradiance is independent of the SZA. The variation in the DGR values at the same SZA interval is caused by changes in the cloud optical depth and in the microphysical properties between different days. Note that although many DGR values are larger than 1, almost all of them are within a $\pm 10\%$ error. This overestimation arises mainly from the correction procedure applied to the measured diffuse irradiances but also from other uncertainties related to the experimental measurements

and unpredictable changes in the atmospheric conditions (ozone, aerosols, etc.).

5.1.3. Cumulus

In agreement with Harrison et al. [15], DGR values for this type of cloud present the greatest variability, which is shown in the large size of the boxes at all SZA. As in the stratocumulus case, this variation is mostly associated with the different cloud optical depths (including those equal to zero when the sun shines between the cloud elements). When the sun is obscured by clouds the direct beam is attenuated and the diffuse component is increased. Thus, the corresponding DGR values are close to 1. On the other hand, when the sun is not occluded by clouds, the direct beam significantly contributes to the global irradiance and the DGR values are close to those for clear sky days. At larger SZAs (low sun) the DGR values show an increment. This fact is mostly related to the increase in the atmospheric path length (Rayleigh scattering) and not necessarily to an effect of cumulus clouds (Mie scattering). This observation is supported by model calculations above clouds (see Section 5.2) and also by the behavior of cirrus and clear sky days on Fig. 4. Although these figures represent different scenarios, both of them show a systematic increase of the DGRs at large SZAs. However, it should be also taken into account that, for cumulus clouds, as the SZA increases the total cloud fraction in a plane perpendicular to the direct beam also increases [26]. As a result, with the increase of the SZA the fractional area of the surface receiving the direct beam irradiance goes down, and hence DGR goes up.

5.1.4. Cirrus

The low dispersion in the DGR values for cirrus clouds determines the small boxes shown in Fig. 4 at all SZAs. The closeness between the DGR values for cirrus and the DGR values for clear days shows that cirrus clouds do not strongly affect the UV-B irradiance at the surface for any SZAs. Thus, the previous general conclusion obtained through the analyzes of the averages and the standard deviations can now be extended to every SZA interval. Once again the increase in the DGR values with the SZA is a consequence of the large atmospheric path length at large SZAs.

5.2. Modeled DGRs: variation with altitude, SZA, and COD

Beyond the specific conditions observed experimentally, it is interesting to evaluate the DGR under all possible conditions. Therefore, TUV model was used to assess the behavior of the DGR when the altitude, the SZA and the COD are simultaneously varied through a more comprehensive range of values.

Here it should be kept in mind that, due to the strong approximations needed to represent clouds in radiative transfer models, the direct comparison against a specific type of cloud is a difficult task. Even though model results are not applicable to some type of clouds (e.g., cumulus), they could have reasonable similarities with those for stratocumulus clouds as they are layered clouds which usually cover the whole sky and have a quite limited vertical development, which lead to a relatively homogeneous radiation field (resembling conditions used in model calculations). For smaller COD, model results could be interpreted as an approximation of the effects of cirrus stratus. In order to capture the details in the variation of the DGRs inside the cloud, a high resolution altitude grid was used for these calculations. In this case, the atmosphere was divided into 800 equally spaced layers (10 m thick) from sea level up to 8 km.

Fig. 5 shows the hourly variation of the DGR for a given day (21 December) at all altitudes below 8 km. Fig. 5(a) shows the DGR for a clear sky day while Figs. 5(b) and (c) show the variation for overcast days with different COD. Fig. 5(a) also shows the SZA variation during the day (dashed line). Calculations were performed at the latitude and longitude of Córdoba with an idealized horizontally homogeneous cloud (denoted by the white horizontal lines) located between 1.5 km and 2.5 km a.s.l. COD ranged from 1 to 30 and cloud properties were considered homogeneous ($g=0.86$; $\omega_o=0.9999$) along its vertical extension. The cloud altitude was selected because it was found to be a frequent height for stratocumulus clouds [27]. The color code in Fig. 5 shows the DGR variation. These panels in Fig. 5 show some interesting features. First, at large SZAs ($\sim 80^\circ$) the DGRs are almost one at all altitudes. As this is true independently of the presence of a cloud, it is clear that it is a consequence of the Rayleigh scattering and the very large path length at these angles. Then, DGR decreases toward solar noon, when the minimum values are found. According to these calculations the minimum DGR expected in Córdoba for a clear day at the surface is 0.4–0.5. As expected the presence of a cloud introduces important changes at all altitudes. Below the cloud, for CODs as low as 5, the DGR at all SZAs is almost 1. Under these conditions no more than 0.6% of the direct beam reaches the surface and only during the noon hours (Fig. 5(b)). Inside the cloud the DGR varies through a wide range of values ($\sim$0.4–1.0). At noon hours and when the COD is low (e.g., 5) this variation is seen along the whole vertical extension of the cloud. If the COD is moderate (e.g., 15) the variation is limited to the first one third of the cloud and above. If the COD is relatively large (e.g., 30, not shown) the variation is restricted to a few hundred meters from the top of the cloud ($\sim$200 m). As the SZA increases, DGRs different from 1 are found only at the highest altitudes (inside the cloud and above). Above the cloud, the effects on the DGR can be seen mainly at solar noon. Observe that as the COD increases, the altitude at which a given DGR is reached also increases. This increase in the diffuse irradiance is observed even at high altitudes and comes from the reflection in the top of the cloud followed by the downward Rayleigh scattering. Despite the Rayleigh scattering is larger at low altitudes, the results described above were not modified when a lower cloud was considered (0.6–1.6 km).

6. Summary and concluding remarks

The effects of different types of clouds (stratocumulus, cumulus, and cirrus) on the broadband UV-B irradiance and on the corresponding DGRs have been analyzed and differentiated by using surface measurements taken in Córdoba City, Argentina.

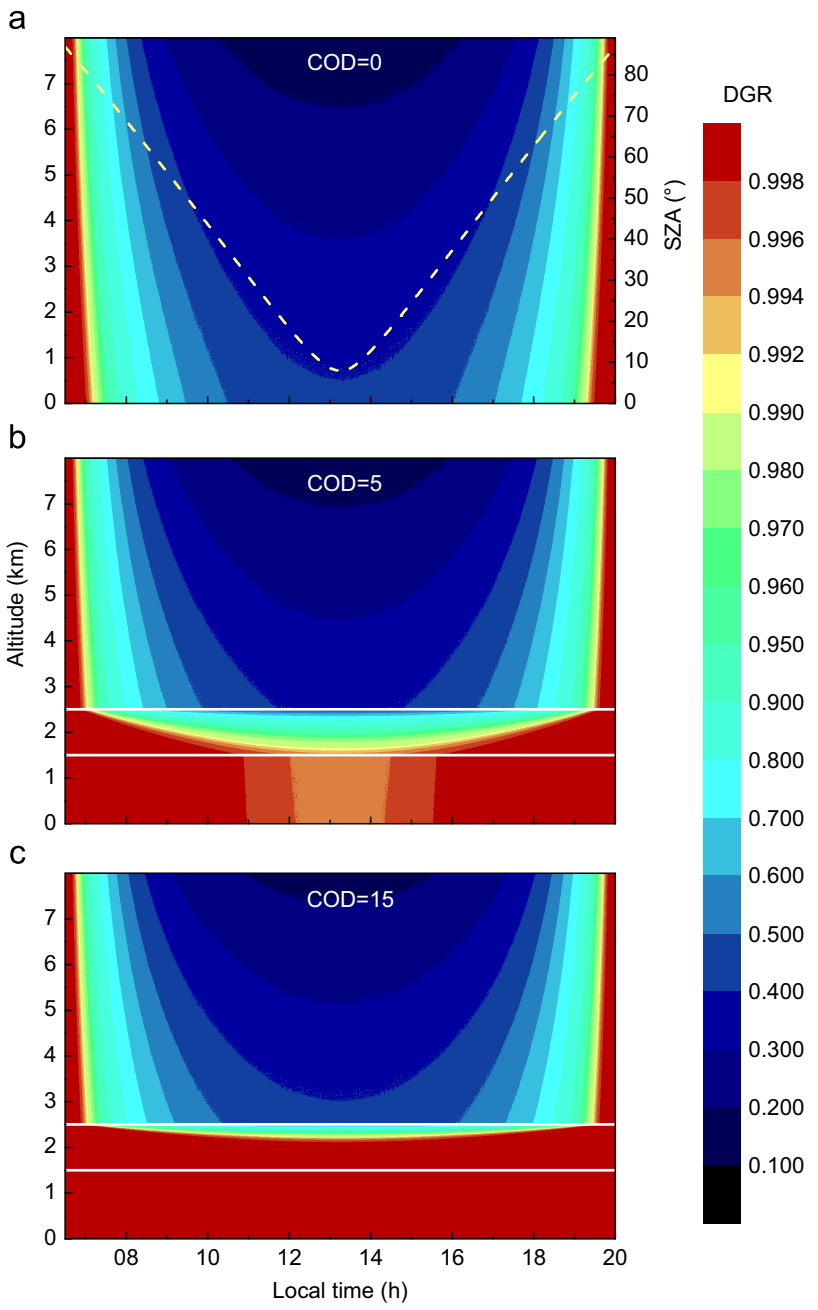

Fig. 5. Model calculations of the hourly variation of the DGR at all altitudes below 8 km for different cloud optical depths. White horizontal lines show the cloud location. Dashed curve shows the SZA variation (right axis).

A total of 16 day with stratocumulus, 12 with cumulus, and 16 with cirrus have been studied using 21 clear sky days as a reference. As has been demonstrated, radiative transfer models are very useful for evaluating cloud effects. Furthermore, the interaction with experimental measurements provides an extremely valuable tool to validate and/or complement the results. In this work it was shown that analyzing the dependence of the DGR with the type of cloud and the behavior of this ratio with altitude, valuable information about the influence of clouds on UV-B irradiance can be retrieved. The TUV model was used to evaluate the DGRs under clear sky conditions and also to assess the effects of an idealized horizontally homogeneous cloud in a wide range of altitudes, SZAs, and cloud optical depths. Although the DGRs are determined by the total optical depth (cloud + aerosol + Rayleigh), the analysis (diffuse and global irradiance, average and standard deviation of the DGRs, and behavior of the DGR as a function of the SZA) led to a clear differentiation of the effects of each type of cloud. The averages and standard deviations for the DGRs were 1.02 ± 0.06 for stratocumulus, 0.74 ± 0.18 for

cumulus, 0.63 ± 0.12 for cirrus, and 0.60 ± 0.13 for the clear sky days, respectively. The results show the large effect of the stratocumulus and the relatively little effect of cirrus on the distribution of the UV-B irradiance at the surface. In addition, stratocumulus clouds showed a low variability in the DGR values, which were concentrated close to at all SZAs. DGR values for cumulus clouds presented a large variability at all SZAs mostly associated with the different optical depths. Finally, the similarity between the DGR values for cirrus clouds and the DGR values for clear days showed that these clouds generally do not strongly affect the UV-B irradiance at surface at any SZA. In general, the radiation path through the cloud (which in turn depends on the SZA, the cloud optical depth, and the morphology of the cloud) determines the distribution of the irradiance components. However, at large SZAs (low sun) the DGRs are mostly determined by the path length through the atmosphere (Rayleigh scattering). In the case of cumulus clouds, as the SZA increases, the DGRs are also affected by the apparent increase in the total cloud fraction. This study was carried out to contribute to the understanding of the radiation–cloud interactions in the UV-B range, a subject of essential importance in the evaluation of photolysis processes and in the development of realistic radiative transfer schemes and chemistry-transport models. The results found in this work will contribute to improve the inclusion of the effect of specific types of clouds in radiative transfer models in order to evaluate photolysis rates under realistic atmospheric conditions. This will be especially useful for the Southern Hemisphere, where measurements are by far less common than in the Northern Hemisphere.

Acknowledgments

We thank CONICET, FONCyT, and SeCyT (UNC) for partial support of the work reported here. María Laura López thanks CONICET for a graduate fellowship.

Appendix A. Diffuse irradiance correction

To correct the measured diffuse irradiance, the measurements from 21 clear sky days were selected along the whole period (14,528 data). In those days, the absence of clouds and aerosols was visually checked by a direct observer and confirmed by comparing the experimental global irradiances against TUV model calculations. The agreement between experimental and TUV-calculated UV-B global irradiances was shown to be better than 10% for SZAs less than 70° [22]. Therefore, it is reasonable to assume a similar agreement for the measured and calculated UV-B diffuse irradiances. Then, the diffuse components for the clear sky days were correlated as is shown in Fig. A1. In this figure, each data set represents a different clear sky day that was fitted with a linear function. All the R-square coefficients for these curves were higher than 0.98. The larger slopes correspond to December–January days (when the lowest value of all minimum SZAs is achieved, around 8°) while the smaller ones correspond to June days. As the slope and the ordinate for each of the

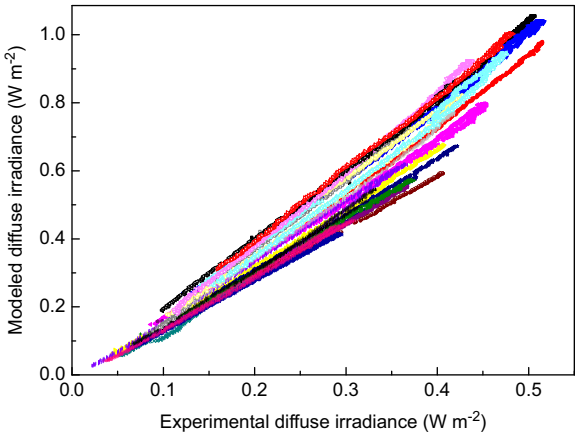

Fig. A1. Correlation between measured and modeled diffuse irradiance. Each data set represents the behavior of a different clear sky day.

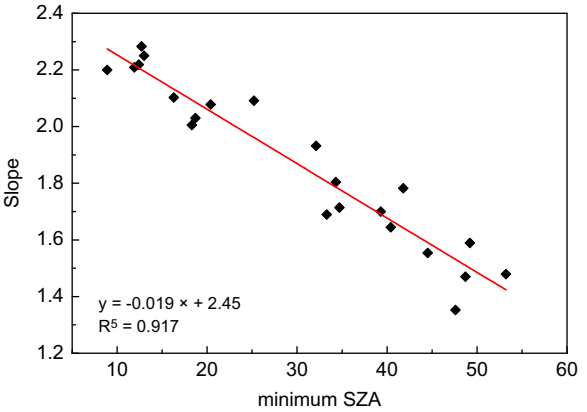

Fig. A2. Correlation between the slopes in plot A1 and the minimum SZA for the corresponding day. The red line shows the linear fit.

observed curves depend on the minimum SZA of the corresponding day (because the inclination of the band was adjusted according to the minimum SZA), these variables were correlated. The results of the slopes and ordinates vs. minimum SZAs are shown in Figs. A2 and A3, respectively. The red lines in these figures are the linear fits. Thus, the procedure followed to correct the diffuse irradiance for a given day is:

1) The minimum SZA of the selected day is calculated.
2) For this SZA the values of the slope and the ordinate are found through an interpolation in plots A2 and A3, respectively.
3) These values determine a linear function where the independent variable is the uncorrected diffuse irradiance and the dependent variable is the corrected diffuse irradiance. Note that the correction does not imply a factor but a function (to consider the variation of the SZA), which will be different for each day.

In our case, most of the diffuse field under the different cloudy conditions was effectively measured. Thus, the assumption that the partitioning of the energy between

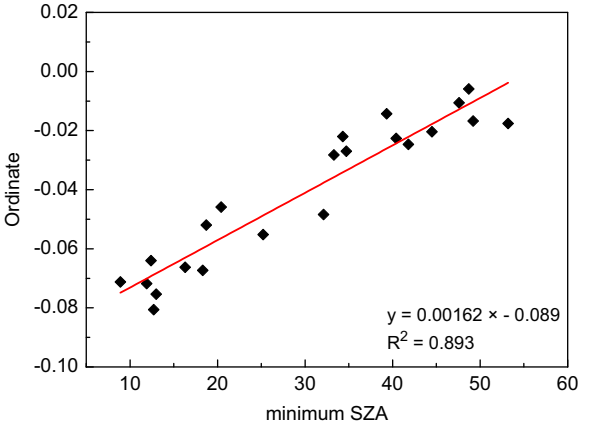

Fig. A3. Correlation between the ordinates in plot A1 and the minimum SZA for the corresponding day. The red line shows the linear fit.

the direct and diffuse components for a clear sky day is equal to that for a cloudy day is only used to take into account the fraction of the diffuse irradiance eclipsed by the band. The uncertainties involved in the described procedure were included in the error bars shown in Figs. 1 and 2.

References

[1] Frederick JE, Snell HE, Hywood EK. Solar ultraviolet radiation at the earth's surface. J. Photochem. Photobiol. 1989;50:443–50.
[2] Matthijsen J, Slaper H, Reinen HAJM. Reduction of solar UV by clouds: a comparison between satellite-derived cloud effects and ground based radiation measurements. J. Geophys. Res. 2000;105: 5069–80.
[3] Díaz JP, Expósito FJ, Torres CJ, Herrera F, Propero JM, Romero MC. Radiative properties of aerosols in Saharan dust outbreaks using ground-based and satellite data: applications to radiative forcing. J. Geophys. Res. 2001;106:18403–16.
[4] Seckmeyer G, Erb R, Albold A. Transmittance of a cloud is wavelength-dependent in the UV-range. J. Geophys. Res. 1996;23: 2753–5.
[5] Koepke P, Reuder J, Schwander H, Solar UV. Radiation and its variability due to the atmospheric components. Recent Res. Dev. Photochem. Photobiol. 2002;6:11–34.
[6] Calbó J, Pagès D, González JA. Empirical studies of cloud effects on UV radiation: a review. Rev. Geophys. 2005;43:1–28.
[7] López ML, Palancar GG, Toselli BM. Effect of different types of clouds on surface UV-B and total solar irradiance at southern mid-latitudes: CMF determinations at Córdoba. Argentina Atmos. Env. 2009;43:3130–6.
[8] El-Nouby Adam M, El Shazly SM. Attenuation of UV-B radiation in the atmosphere: clouds effect, at Qena (Egypt). Atmos. Env. 2007; 41:4856–64.
[9] Simic S, Fitzka M, Schmalwieser A, Weihs P, Hadzimustafic J. Factors affecting UV irradiance at selected wavelengths at Hoher Sonnblick. Atmos. Res. 2011;101:869–78.
[10] Sabburg J, Calbó J. Five years of cloud enhanced surface UV radiation measurements at two sites (in the Northern and Southern Hemispheres). Atmos. Res. 2009;93:902–12.
[11] Kanaya Y, Kajii Y, Akimoto H. Solar actinic flux and photolysis frequency determinations by radiometers and a radiative transfer model at Rishiri Island: comparisons, cloud effects, and detection of an aerosol plume from Russian forest fires. Atmos. Env. 2003;37: 2463–75.
[12] Ogunjobi KO, Kim YJ, He Z. Influence of the total atmospheric optical depth and cloud cover on solar irradiance components. Atmos. Res. 2004;70:209–27.
[13] Jacovides CP, Tymvios FS, Assimakopoulos VD, Kaltsounides NA. The dependence of global and diffuse PAR radiation components on sky conditions at Athens. Greece Agric. Forest Meteorol. 2007;143: 277–87.
[14] Kaskaoutis DG, Kambezidis HD, Kharol SH. Badarinath KVS. The diffuse-to-global spectral irradiance ratio as a cloud-screening technique for radiometric data. J. Atmos. Solar-Terrest Phys. 2008;70:1597–606.
[15] Harrison RG, Chalmers N, Hogan RJ. Retrospective cloud determinations from surface solar radiation measurements. Atmos. Res. 2008;90:54–62.
[16] Long CN, Ackerman TP. Identification of clear skies from broadband pyranometer measurements and calculation of downwelling shortwave cloud effects. J. Geophys. Res. 2000;105:15609–26.
[17] Junkermann W. The actinic UV-radiation budget during the ESCOMPTE campaign 2001: results of airborne measurements with the microlight research aircraft D-MIFU. Atmos. Res. 2005;74: 461–75.
[18] Podgorny IA, Li F, Ramanathan V. Large aerosol radiative forcing due to the 1997 Indonesian Forest Fire. Geophys. Res. Lett. 2003;30:1028–31.
[19] Diner DJ, Braswell BH, Davies R, Gobron N, Hu J, Jin Y, et al. The value of multiangle measurements for retrieving structurally and radiatively consistent properties of clouds, aerosols, and surfaces. Rem. Sens. Env. 2005;97:495–518.
[20] Pfister G, Baumgartner D, Maderbacher R, Putz E. Aircraft measurements of photolysis rate coefficients for ozone and nitrogen dioxide under cloudy conditions. Atmos. Env. 2000;34:4019–29.
[21] Palancar GG, Toselli BM. Erythemal ultraviolet irradiance in Córdoba, Argentina. Atmos. Env. 2002;36:287–92.
[22] Palancar GG, Toselli BM. Effects of meteorology on the annual and interannual cycle of the UV-B and total radiation in Córdoba City, Argentina. Atmos. Env. 2004;38:1073–82.
[23] Madronich S. Photodissociation in the atmosphere: 1. Actinic flux and the effects of ground reflections and clouds. J. Geophys. Res. 1987;92:9740–52.
[24] Stamnes K, Tsay SC, Wiscombe W, Jayaweera K. A numerically stable algorithm for discrete-ordinate-method radiative transfer in multiple scattering and emitting layered media. Appl. Opt. 1988; 27:2502–9.
[25] Olcese LE, Toselli BM. Some aspects of air pollution in Córdoba, Argentina. Atmos. Env. 2002;36:299–306.
[26] Várnai T, Davies R. Effects of cloud heterogeneities on shortwave radiation: comparison of cloud-top variability and internal heterogeneity. J. Atmos. Sci. 1999;56:4206–24.
[27] Zuidema P, Painemal D, De Szoeke S, Fairall C. Stratocumulus cloud top height estimates and their climatic implications. J. Clim. 2009; 22:4652–66.